Metal-insulator transition in *trans*-polyacetylene

E. M. Conwell, H. A. Mizes, and S. Jeyadev
Xerox Corporation, Webster Research Center (0114-40D), 800 Phillips Road, Webster, New York 14580
(Received 3 March 1989)

We have calculated the band structure for a chain of doped *trans*-polyacetylene using the electronic part of the Su-Schrieffer-Heeger Hamiltonian plus the Coulomb potential arising from ions and charged solitons surrounding the chain. The lattice structure used was that determined by x rays for Na-doped polyacetylene. To agree with a number of experimental observations the donated electrons were taken to be in soliton states at all dopant concentrations. In obtaining the potential of a point charge on a chain in the metallic state, the confinement of the free electrons to a chain was taken into account. Because screening depends on the calculated energy levels, specifically on the density of states at the Fermi energy, $\eta(E_F)$, in the metallic state, which, in turn, depend on the potential used to obtain them, self-consistency was required in the calculations. The energy-level structure was found to depend strongly on the ion spacing, conveniently measured in terms of the average spacing a of C—H's along the chain. For ion spacing $5a$, characteristic of the Na-ion-rich regions up to an average dopant concentration of $\sim 6\%$, the chain remained semiconducting. For ion spacing $4a$, which appears to characterize the next phase for Na doping, metallic behavior was found for a doped chain length of ~ 100 sites or more. Self-consistency was fulfilled with $\eta(E_F)$ equal to the value obtained from the saturation spin susceptibility in the metallic state. In addition to sufficiently long chains that the level spacing is comparable to kT, the metal-insulator transition is found to require considerable overlap of electron wave functions on adjacent solitons and a fairly deep potential well. The transition is best described as a Mott transition. Our model predicts that a sample in the metallic state at room temperature becomes semiconducting at lower temperature. Evidence for this is found in the temperature variation of the spin susceptibility and of ESR linewidth. It is argued that the energy-level distribution in the metallic state is similar for other dopants. We show also that our model is consistent with the optical absorption observed for doped polyacetylene.

I. INTRODUCTION

trans-polyacetylene, to be abbreviated $(CH)_x$, when undoped has very low conductivity and a gap of ~ 1.8 eV. With doping the conductivity rises, very rapidly up to a concentration of $y \sim 1\%$ and then less rapidly with further increase in y. Doping-induced absorption over a wide range of frequencies in the gap appears for y as small as 0.3% with a gentle maximum around midgap, and increases with y.[1] At $\sim 6\%$ doping the original gap has disappeared.[1] Temperature-independent susceptibility, i.e., Pauli susceptibility, is quite small for small y and shows a strong increase around 4–6 % doping. The details of the increase of the Pauli susceptibility, χ_P, with y are quite dependent on the dopant and the sample treatment. It is generally found, however, that for $y \sim 4$–6% χ_P has increased to within a factor 2 of the value that would be obtained if all the π electrons were conducting, i.e., if the gap in the π band had disappeared, the bandwidth remaining constant. The increase in χ_P with y is particularly striking for Na-doped[2] and ClO_4-doped[3] $(CH)_x$, where χ_P, for carefully prepared samples, goes from $<1\times10^{-8}$ to $\sim 2\times10^{-6}$ emu/mol in the range $\sim 5\% < y < 7.5\%$. Because the gap in the optical absorption has essentially disappeared at $y \sim 6\%$ and the conductivity is quite high, the rapid rise in χ_P is taken to indicate an "insulator-metal" transition. It has been proposed that this transition is first order.[4]

It is generally accepted that donation of an electron or hole to a $(CH)_x$ chain results in chain relaxation. When two or more electrons or holes are added, the relaxation takes the form of charged soliton states.[1–4] Evidence that this is the case, at least up to 4–6 %, is the small value of χ_P mentioned above, resulting from the pairing of electrons or holes in the charged solitons.[2–4] Early attempts to account for the insulator-metal transition showed that a highly disordered arrangement of the doping impurities would cause the soliton levels to spread throughout the gap, quenching the Peierls distortion, at high enough concentration.[5,6] Another attempt to explain metallic behavior was based on strong disorder causing a transition to an incommensurate Peierls state with a large density of states in the gap.[7]

A serious difficulty with transition mechanisms based on disorder is that structure studies by x-rays, neutron scattering, and electron scattering establish that above doping levels $\sim 0.4\%$ the impurities, although concentrated in a second phase, are quite well ordered within that phase.[8,9] In Na-doped $(CH)_x$, in particular, the regular arrangement of ions, plus the small χ_P below $\sim 6\%$ doping, suggested the existence of a soliton lattice in the impurity-rich phase for $y \lesssim 6\%$.[2,3] The steep increase in χ_P above $\sim 5\%$ doping led to the proposal that the insulator-metal transition is a phase transition from a sol-

iton to a polaron lattice.[10] A strong argument against this suggestion is the fact that the intensities of the three doping-induced infrared-absorption lines [infrared-active vibrational (IRAV) modes], established as being due to solitons at low concentrations,[11,12] have been found to increase more or less linearly with ion concentration in K-doped $(CH)_x$ up to $\sim 18\%$;[13] theoretical calculations have shown that these absorptions should be quite unobservable for a polaron lattice at high concentrations.[14,15] Further, electron-energy-loss experiments on heavily-Na-doped $(CH)_x$ show levels spread well across the gap,[16] whereas a polaron lattice would result in two narrow well-separated bands in the gap. It was pointed out by Fink *et al.*[16] that the energy-level distribution they find is consistent with the electrons remaining in soliton states. Persistence of soliton states should give rise to sufficient variation of the charge density along the chains even at large y to explain the observation of IRAV to 18% K doping. We conclude on these various grounds that the insulator-metal transition does not involve a change in the nature of the lattice relaxation; the soliton lattice exists for y values above as well as below the transition.

Even though the carriers go into a soliton lattice, the usual theories for the amplitude soliton lattice[17] or the phase-amplitude soliton lattice[18] are not applicable because these theories neglect the effects of the ions. In these theories the spacing of solitons is determined solely by the number of electrons added to the chain, so that as y increases the soliton spacing decreases steadily. In practice, because of the two-phase nature of doped $(CH)_x$, the spacing of solitons in the doped phase remains constant over wide ranges of y because the ion spacing remains constant, an increase in y resulting in an increase in the doped chain length.[19] The soliton-lattice theories[17–19] also neglect the Coulomb potential of the ions, as, in fact, do all the theories mentioned above, with the exception of that in Ref. 5. With the ions located between the $(CH)_x$ chains and typically having a periodicity $3a$ to $5a$, where a is the average distance between CH groups, this potential is clearly large. Calculations of Bryant and Glick for a single impurity ion approximately halfway between chains show that the potential of the ion has a strong effect on the distribution of energy levels in the conduction and valence bands.[20] Actually, the effects are considerably larger than calculated by them because they assumed an isotropic dielectric constant ϵ of 10, whereas the transverse dielectric constant, in particular, is much smaller. As a result of the ion potential, several levels are pulled into the gap, and the location of soliton or polaron levels is strongly affected.[20,21] Thus it is essential to include the ion potential in band-structure calculations. Neglecting the ion potential, Stafström and Brédas[19] found a large gap between the soliton band and both valence and conduction bands to be maintained beyond 6% doping.[22] In the calculations of Bulka,[23] the effect of the ion potential was limited to the nearest-neighbor C atom to a dopant ion. Here also the gap was not found to disappear, even at high dopant concentrations.

We have done band-structure calculations for a doped $(CH)_x$ chain with the electrons in soliton states and the ion potential plus the potential due to solitons on nearby chains included.[24] We did indeed find the gap to disappear for a structure approximating that found for Na-doped $(CH)_x$ by x rays, a reasonable value of chain length, and a y value in accord with experimental data.[24] In this paper we carry these calculations further by using the actual structure found for Na-doped $(CH)_x$ and doing a more careful treatment of screening. It is clear that with the ions and other charged solitons so close to the $(CH)_x$ chain, an accurate treatment of screening is important. For undoped polyacetylene the screening at long distances from a charge is given by the dielectric-constant tensor, for which the most recent values are $\epsilon_{\parallel}=11.5$ (Ref. 25) and $\epsilon_{\perp}=2.5$.[26] Close to the charge the screening is less, i.e., the potential greater, than these values would indicate. With increasing doped chain length the gap tends to decrease.[24] A decrease in gap would make the dielectric constant increase.[27] Since the gap is dependent on the potential, an accurate determination of the variation of the gap with doped chain length requires, in general, a difficult self-consistent calculation. Fortunately, when the chain is in the metallic state, the problem is more tractable because screening depends only on $\eta(E_F)$, the density of states at the Fermi energy. Self-consistency then requires that $\eta(E_F)$ obtained from the band-structure calculation agree with $\eta(E_F)$ introduced initially in determining the screening. As will be shown, such a self-consistent calculation leads again to the metallic state occurring at reasonable chain length and a doping concentration in accord with experiment. For the doping concentration characteristic of the nonmetallic phase in Na-doped $(CH)_x$, we also obtain reasonable self-consistency in that the gap changes calculated using the ϵ values for pristine material are quite small.

The plan of this paper is as follows. In Sec. II we describe our band-structure calculations and results. The following section begins with the derivation of the dependence of the spin susceptibility on properties of the chain and the temperature T. Because the chain lengths at which metallic susceptibility is predicted at 300 K are relatively short, ~ 100 C—H's, the spacing between levels at the Fermi energy is still approximately the thermal energy (kT) at 300 K. Thus our model predicts that, as the temperature is lowered, the "metal" will revert to a semiconducting state. Experimental evidence for this reversion, from studies of ESR linewidths[28] and the temperature dependence of χ, will be given in Sec. III. In Sec. IV we discuss the sample and dopant dependence of the insulator-metal transition, as seen in susceptibility and x-ray measurements. In Sec. V we describe how our model accounts for the observed variation of the optical absorption with doping. Finally, we summarize our results and conclusions in Sec. VI.

II. BAND-STRUCTURE CALCULATIONS

A. Hamiltonian

The Hamiltonian used for these calculations was the electronic part of the Su-Schrieffer-Heeger (SSH) Hamil-

tonian[29] plus the Coulomb potential of ions and solitons, i,e.,

$$H=-\sum_{n=1}^{N-1}[t_0+\alpha(u_n-u_{n+1})](c_{n+1}^{\dagger}c_n+\text{H.c.})+\sum_{n=1}^{N}V_n c_n^{\dagger}c_n \ . \quad (1)$$

Here, u_n is the displacement of the nth lattice site, t_0 the transfer or overlap integral when $u_n=0$ for all n, α the rate of change of the overlap integral with distance between nearest neighbors, $c_n^{\dagger}$, and c_n creation and annihilation operations for a π electron on the nth site, and N the number of sites on the chain. V_n is the sum of the Coulomb potential due to the ions and solitons on the other chains. We neglect the contribution of solitons on the chain being calculated for because their potentials should be strongly screened. For simplicity, the solitons on the other chains were assumed to be point charges.

The presence of N_s solitons on the chain was incorporated by taking

$$u_n=-(-1)^n u_0\prod_{j-1}^{N_s}\tanh\left[\frac{n-jb}{l}\right], \quad (2)$$

where u_0 is the displacement in the perfectly dimerized chain, b the spacing between soliton centers, and l the half-length of a soliton.

B. Structure

The relative locations of ions and $(CH)_x$ chains, shown in Fig. 1, were taken to be those found in x-ray investigations of Na-doped $(CH)_x$.[30] In earlier calculations[24] we assumed a structure in which the equilateral triangles were aligned base to base rather than apex to base as in Fig. 1, so that the center $(CH)_x$ chain, for which the calculations were done was the common base for two triangles. As a consequence, the two closest ion columns were at a distance d from the center chain, rather than at d and $2d$, as in Fig. 1, and there were four nearest-neighbor solitons rather than six. Each of the six nearest-neighbor solitons is at a distance $d\sqrt{3}$ from the center of the chain for which the calculations were done. The distance d was taken as 2.4 Å,[31] in close agreement with 2.26 Å found between Na^+ ions and graphite planes in intercalated graphite.[32] Calculations were also done for charges more remote than nearest neighbors, as will be discussed.

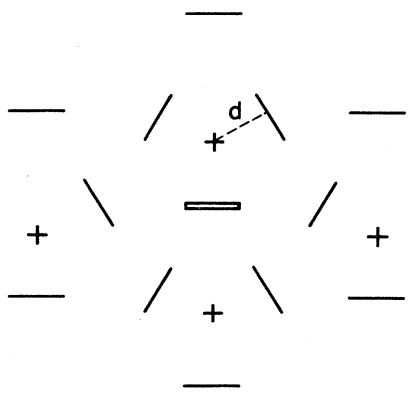

FIG. 1. End-on view of a portion of the polyacetylene structure used for calculations. Each $(CH)_x$ chain lies along the side of an equilateral triangle with the ion column, indicated by +, at a distance d from each of the three chains surrounding it. The double line indicates the chain for which the calculations were done. The two nearest ion columns and the six nearest solitons will be referred to as the first shell of charge, the next-closest pair of ion columns and set of six solitons the second shell of charge, etc. The first and second shells are displayed in the figure.

The existence of different phases for different doping ranges has been established by x rays[8,9] and electrochemical measurements.[33] For Na doping with average concentration $\langle y\rangle$ between $\sim 0.4\%$ and $\sim 6\%$, the spacing between ions in a column is $5a$.[33] With three $(CH)_x$ chains per Na column, the distance b between soliton centers in this phase is $15a$ and the actual Na concentration in the phase is 6.67%. The ion spacing in the next ordered phase is not as clear. According to the discussion of Ref. 33, a spacing of $4a$ seems most likely, although it is not possible to rule out $3a$ or a combination of $4a$ and $3a$. We have taken the value $4a$, for which we believe, as will be discussed in Sec. IV, there is further evidence. That choice makes the spacing between soliton centers in this phase $12a$, corresponding to $y=8.33\%$. As a consequence of the even spacing, alternation of solitons and antisolitons requires alternation of the usual soliton having (schematically) two single bonds at its center with one having two double bonds at its center. Within the SSH treatment, where Coulomb forces between the electrons in the soliton are neglected, these two solitons have the same energy. Close equality of the energy for the two configurations has also been shown using the Pariser-Parr-Pople (PPP) model.[34]

According to Refs. 2–4, the increase in χ_P, and thus the transition to the metallic state, begins at an average concentration of $\sim 6\%$. Because $(CH)_x$ samples are never completely doped, presumably due to the presence of amorphous regions and other defects, this suggests that at $\langle y\rangle \sim 6\%$ as much of the sample as can be doped has a concentration 6.67%. The rise in χ_P starting at $\sim 6\%$ then corresponds to the buildup of the next phase, which we have taken as 8.33%. Because the states are widely separated in energy for short chain lengths, the attainment of metallic properties must require a sufficient length of chain, L_d, doped to 8.33%. The determination of L_d is one objective of these calculations. It is to be expected that $L_d \sim 100a$ because there is no evidence for coherence lengths much longer than this by any measure.

C. Calculations with dielectric screening

We will first consider the case of 6.67%, corresponding to an ion spacing of $5a$. From the above discussion it is reasonable to assume, at least for a first iteration, that there is dielectric screening, with the ϵ values those cited earlier for pristine material. The Coulomb potential is

then given by[24]

$$V_n = -\sum_i \frac{ee_i}{\epsilon_\perp[(n-n_i)^2a^2+(\epsilon_\parallel/\epsilon_\perp)R_i^2]^{1/2}}, \quad (3)$$

where $-e$ is the charge on the electron, $\pm|e_i|$ the ith charge, n_i the site on the chain that the ith charge is opposite, and R_i the perpendicular distance of the charge from the chain. For the calculation of V_n, the "phase," or the arrangement of the solitons, on each chain was taken to be determined by the position of the chain in its equilateral triangle. Thus, for example, the soliton centers would be located at the same set of sites on each chain that forms the base of an equilateral triangle in Fig. 1, while for the chains that form the left and right sides of the triangles the soliton centers would all be shifted by five sites ahead and behind, respectively.

In calculating the energy levels from Eqs. (1)–(3), we took the energy gap ($\equiv 2\Delta$) to be 1.8 ev, $u_0=0.035$ Å, $t_0=2.5$ eV, $a=1.22$ Å, and $d=2.4$ Å. Consistent with these values and the SSH Hamiltonian α ($=\Delta/4u_0$) (Ref. 29) was taken at 6.42 eV/Å and the soliton half-width l ($=2t_0/\Delta$) (Ref. 35) at 5.5 sites. Although it has been shown that the soliton half-width is decreased below $2t_0/\Delta$ in the presence of a single ion,[29] a decrease does not appear likely when there is a row of closely spaced ions. Calculations were done for chain lengths corresponding to $2m$ solitons, $6m$ ions, and chain lengths of $(2m+1)b$ sites for odd b, $(2m+1)b-1$ sites for even b, and m values 1–10. For every value of m, $2m$ soliton levels are introduced in the gap. If the Coulomb potential due to the ions and other solitons is neglected, the soliton levels, conduction band, and valence band are symmetric about midgap. Because the soliton levels are taken from the conduction and valence bands, the gap between the bands widens somewhat in the presence of the solitons. The gap of significance now, however, is the energy interval between the top soliton level and the conduction-band edge. We find from Eqs. (1) and (2) that for 6.67% and $V_n=0$ the gap varies from 0.875 eV for two solitons to 0.716 eV for eight solitons (134 sites). With the inclusion in the Hamiltonian of V_n given by Eq. (3), for $\epsilon_\parallel=11.5$ and $\epsilon_\perp=2.5$, we found little decrease in the gap, ~ 0.02 eV for a 134-site chain, and less for shorter chains. In these calculations we included charges out to the second shell (see Fig. 1), but there was not a significant change between the values calculated with the first shell only and those calculated going as far as second, third, or fourth shells.

One reason that the effects on the energy levels are much smaller than those calculated for a single ion is that the positive potentials due to the ions are strongly compensated by the negative potentials due to the solitons. The degree of compensation has been overestimated in the calculation described above, however, by not allowing for the variation of ϵ, with distance, i.e., the incomplete screening close to a charge. Calculations by Resta, for example, for diamond, Si, and Ge show that the full value of ϵ is not attained until the distance from a point charge is about equal to the interatomic spacing.[36] Thus, in particular, we have overestimated the screening of the positive ion column closest to the chain. Resta's calculations were done for cubic crystals and are, unfortunately, much more difficult to do for a uniaxial crystal. To obtain an estimate of the effect of the diminished screening, we assumed, in the spirit of Resta's results, that each component of ϵ varies linearly from unity at the ion to its full value (11.5 or 2.5) at one interatomic distance, equal to 1.22 Å along the chains and 4.16 Å perpendicular to the chains. These calculations led to slightly larger gaps rather than the smaller gaps expected; in fact, they tended to restore the gap calculated without the Coulomb potential. The numerical calculations of the variation of the gap with increasing Coulomb potential, to be described later, show that this is typical behavior when V_n is small. We conclude that at 6.67% doping $(CH)_x$ remains a semiconductor with gap changed little by the Coulomb potential. It is not certain that we have done a self-consistent calculation; the dielectric constant used was that for pristine rather than doped material. However, we see no possibility for the dielectric constant to change greatly, and thus none for the gap to be changed much at the 6.67% concentration.

For 8.33% doping, according to the earlier discussion, it is expected that the gap will not be decreased much by the Coulomb potential at short chain lengths, so that the dielectric constants for pristine material should still be more or less valid. The calculated results for chains of two and four solitons are consistent with this expectation. For four solitons, with the ϵ values taken as constants, the gap decrease is only 0.01 eV. Allowing the ϵ values to decrease as discussed above near the closest positive ions resulted in a gap decrease of 0.08 eV, still not a large decrease. For longer chains the gap decreases grow larger and it becomes necessary to take into account the variation of dielectric constant with the change in gap. We note that initially the expected increase in ϵ with decreasing gap, which decreases the Coulomb potential, should have the effect of slowing the gap decrease with increasing chain length. Thus when a self-consistent calculation is done, the transition to the metallic state with increasing chain length might be relatively abrupt.

D. Metallic screening

We now turn to the metallic region where, as indicated earlier, a self-consistent calculation is feasible. Primary consideration must be given to the screening. As pointed out for the dielectric case, with the potentials of positive and negative charges tending to cancel each other, the detailed variation of screening with distance close to a charge is very important in determining V_n. An essential complication here is that free carriers confined to chains are less effective in screening than those that can move freely in three dimensions. Thus a point charge on a chain will be screened very little outside the chain by the motion of carriers within the chain because the electronic charge is essentially unable to adjust by lateral motion to the presence of the test charge.[37] The test charge is nevertheless screened in a material with an assembly of parallel chains because the carriers can move between the surrounding chains, by hopping, tunneling, or drift if the

transverse transfer integral is large enough.[38] Although the time scale for such motions could be long, they would certainly contribute to static screening. To describe static screening in a sample made up of metallic chains, Davis therefore set up a model in which the chain with the point charge, represented as a cylinder with radius R_1, is surrounded by empty space up to a radius R_2, while the space for $R \geq R_2$ is filled by a coaxial metallic cylinder representing all the other chains.[38] R_2 is chosen as the distance between nearest-neighbor chains. In a Thomas-Fermi semiclassical treatment, Poisson's equation for the ith of the three regions into which space has been divided is

$$\nabla^2 V = \kappa_i^2 V \ , \tag{4}$$

where κ_i is the inverse screening length in the ith region, given by

$$\kappa_i^2 = 4\pi e^2 \eta_i(E_F) \ . \tag{5}$$

The general solution of Poisson's equation for the ith region is[38]

$$V_i(R,z) = \int_{\alpha=0}^{\infty} [A_i(\alpha) I_0(\beta_i R) + B_i(\alpha) K_0(\beta_i R)] \cos(\alpha z) d\alpha \ , \tag{6}$$

where I_0 and K_0 are the modified Bessel functions of order zero, $\beta = (\kappa_i^2 + \alpha^2)^{1/2}$, and $A_i(\alpha), B_i(\alpha)$ are coefficients to be determined by the boundary conditions at $R = 0, R_1, R_2$.

Evaluation of the potential must be carried out numerically. R_2, the radius of the outer metallic cylinder, was taken as the distance between nearest-neighbor $(CH)_x$ chain centers, which, as shown in Fig. 1, is $d\sqrt{3} = 4.16$ Å. To obtain κ in the outer, metallic cylinder we used the density of states at the Fermi energy deduced from measurements of the Pauli susceptibliity in the metallic state, 0.08 states/eV C-atom.[2] This value led to $\kappa = 0.87/\text{Å}$, essentially a bulk screening value, for the outer cylinder. To ensure that the inner cylinder contributes very little to the screening, as required on physical grounds, the calculations were done with successively smaller values of R_1. For $R_1 \leq 0.002$ Å there was very little effect on the potential of the choice of R_1; thus R_1 was taken as 0.002 Å. κ_i inside the central chain differs from κ_i in the outside cylinder because the density of carriers in the chain is different from that in the metallic region, which is taken as the density of π electrons. (We neglect the donated electrons, which are $< 8.5\%$ of the π electrons.) Inside the central chain the density of carriers is $1/\pi R_1^2 a$, a being 1.22 Å. Making use of the fact that $\eta(E_F)$ is proportional to the cube root of carrier concentration, we find κ_i inside the chain to be ~ 10.3 times κ_i in the outside cylinder, or 9.0/Å. The calculated potential versus distance due to a point charge in metallic polyacetylene that results from these values is shown in Figs. 2 and 3. At small distances from the charge the potential approaches the unscreened, spherically symmetric Coulomb value, $\pm e^2/(R^2+z^2)^{1/2}$. With increasing distance from the charge, the potential falls below the Coulomb value. This occurs at distances smaller than that to the nearest chain, 4.16 Å, as discussed earlier. Beyond the nearest chain the potential is seen to fall off more rapidly, approaching asymptotically the dependence $e^{-\kappa R}$, with $\kappa = 0.87/\text{Å}$, the bulk screening value, in the plane containing the point charge perpendicular to the chain. The rate at which the potential falls with distance is less rapid for directions at an angle to the transverse plane, according to Fig. 3; this is an expected result of the confinement of the carriers to chains.

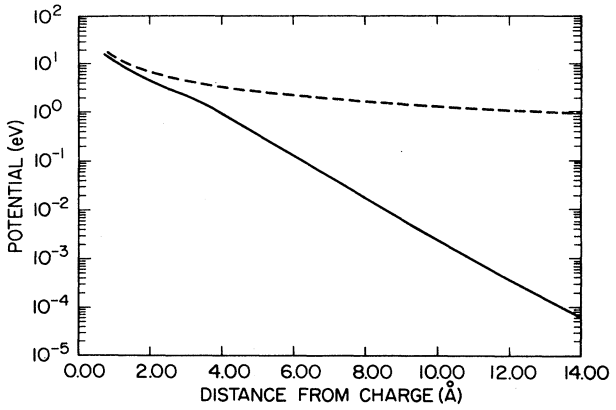

FIG. 2. Potential for a point charge e on a chain in metallic $(CH)_x$ vs distance from the charge in the plane perpendicular to the chain for no screening (— — —) and Davis screening with $R_2 = 4.16$ Å, $\kappa_2 = 0.87/\text{Å}$.

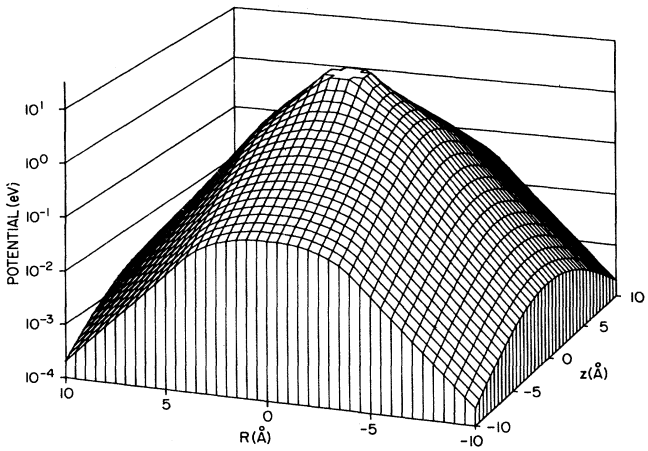

FIG. 3. Potential for a point charge e on a chain in metallic $(CH)_x$ vs distance from the charge in a plane containing the chain. The calculations were done using Davis screening with $R_2 = 4.16$ Å, $\kappa_2 = 0.87/\text{Å}$.

E. Band structure in the metallic range

We now calculate the band structure of a chain containing eight solitons (108 sites) with spacing $b=12$ (8.33% doping), assuming that the screening is metallic with $\eta(E_F)=0.08$ states/eV C-atom. In Sec. IV we will show that a calculation of the density of states for the resulting band structure leads to the same $\eta(E_F)$, making the calculation self-consistent. Thus chains of 108 sites or more with 8.33% doping will exhibit so-called metallic behavior of χ_P.

In Fig. 4 is shown the potential V_n calculated for a chain of 108 sites containing eight solitons, surrounded, according to the geometry of Fig. 1, by similar $(CH)_x$ chains and by ion columns of 24 ions spaced $4a$ apart. Ions and solitons were all treated as point charges with potentials versus distance given by Figs. 2 and 3. For the calculation of V_n, charges out to the fourth shell were included. It was found that V_n is mainly determined by the first shell. The next shell of charge did have some effect on the gap and the $\eta(E_F)$ ultimately obtained, but further shells of charge had little effect, as anticipated from the exponential falloff of the point-charge potential with distance shown in Figs. 2 and 3.

It is seen in Fig. 4 that the potential well has an average depth of ~ 3 eV, with oscillations of amplitude 1.3 eV. The sharp minima of V_n occur at the soliton centers where the positive potential energy due to the off-chain solitons is a minimum. The maxima occur at the sites halfway between solitons on the other two chains in the triangle, where their potential energy is a maximum. Thinking that the maxima and minima would be less sharp if the soliton charges had not been assumed to be point charges, we redid the calculations with the electrons spread out, self-consistently. This affected the potential very little, the changes being of the order of a few percent. In any case, we have been able to show that the energy levels depend little on the height of the fluctuations, but are determined mainly by the well depth and shape of the well at the ends. It may be noted that the height of the fluctuations is very much less for the dielectric-screening case, where the potential falls off inversely with distance rather than exponentially.

The energy levels calculated for the potential of Fig. 4 are given at the extreme right of Fig. 5. To show how these levels evolve as the Coulomb potential increases from zero, they are plotted as a function of the fraction of the Coulomb potential. In other words, it is considered that the Coulomb potential is given by fV_n and the plot in Fig. 5 shows the level evolution as f increases from 0 to unity. It is seen that with the increase of f from zero, the levels tend to separate in groups of eight, or multiples thereof, as a result of the presence of eight solitons. At very low values of f, eight localized levels separate off from the bottom of the valence band. The progressively greater electron concentration at the center of the chain for these states with increasing potential results in greater electron concentration at the ends of the chain for states at the top of the valence band. Finally, two of the top states are sufficiently concentrated at the edge of the well that they can no longer lose energy with further increase in f and they separate from the top of the valence band. While they are in the gap the states stay localized at the ends of the chain. When the pair joins the soliton band, the wave functions are again delocalized throughout the chain. As the fraction of the potential increases from zero, levels separate from the top of the soliton band and the top of the conduction band for the same reason as just described for the pair at the top of the valence band, going through the same types of change in their wave

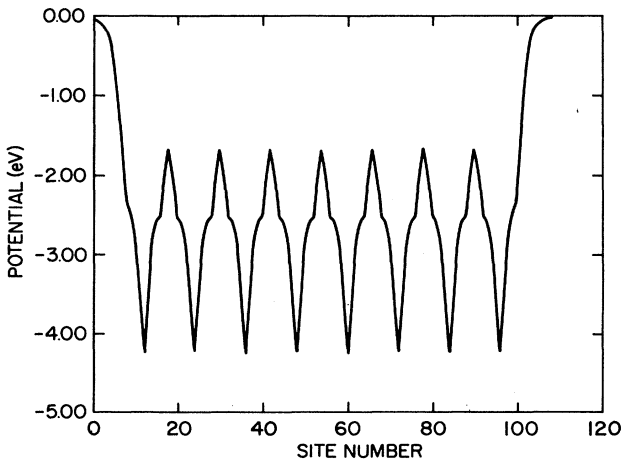

FIG. 4. Potential energy V_n vs site number calculated using the potential of Figs. 2 and 3 for a $(CH)_x$ chain of 108 sites with eight solitons, centers 12 sites apart, surrounded, as shown in Fig. 1, by similar $(CH)_x$ chains and ion columns of 24 ions with spacing $4a$.

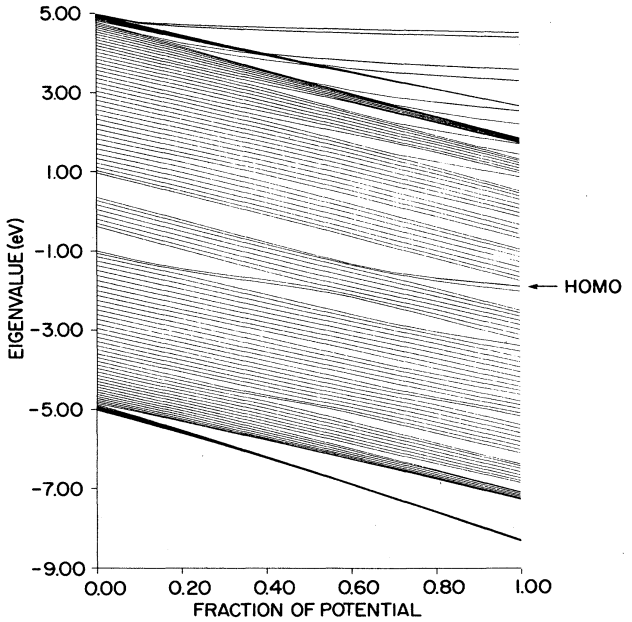

FIG. 5. Calculated energy levels for the case of Fig. 4 as a fraction of the potential shown there.

functions as described for that case. The most significant change for the properties of the material is the separation of the two highest occupied states from the soliton band to join the conduction band at the full value of the potential. The highest occupied level, indicated by an arrow in Fig. 5, is then 0.142 eV below the next level. This spacing is seen to be of the order of the spacing between conduction-band levels, although slightly larger. The eigenfunction for this level is somewhat asymmetric, as indeed all the eigenfunctions are because the potential was slightly asymmetric for the $b=12$ spacing, but it clearly does not represent a localized state.

In the next section we will derive the relation between χ_P and the energy-level distribution around E_F. It will be shown that the distribution of Fig. 5 leads to $\eta(E_F)=0.080$ states/eV C-atom at room temperature, thus satisfying the self-consistency condition. With the chain length, 108 sites, a reasonable average length for coherent doping, it appears that Fig. 5 gives a good description of the energy levels in the metallic state.

In addition to sufficiently long chains, achievement of the metallic state requires both good wave-function overlap in the soliton states and a deep potential well. Evidence for the former requirement is provided by a calculation for 6.67% doping with eight solitons (134 sites) and metallic screening. The potential was very similar to that shown in Fig. 4, having also a well depth $\simeq 4$ eV, but the calculated gap between the highest occupied and lowest empty levels was 0.43 eV. The big difference between the 6.67% case and the 8.33% case is poor wave-function overlap for the former, with the soliton length, $\simeq 2l$, equal to 11 sites, while the distance between soliton centers is 15 in the 6.67% case and 12 in the 8.33% case. The requirement of a deep potential well is demonstrated by calculations for 8.33% with everything identical to that discussed above, except that V_n was calculated assuming dielectric screening, i.e., $\epsilon_{\parallel}=11.5$ and $\epsilon_{\perp}=2.5$. As was found also for the calculations with shorter chains, this leads to a well depth ~ 1 eV. Even with the soliton length $2l$ taken as 14, a gap of 0.39 eV remained for the 8.33% case with 10 solitons, a chain length of 132 sites, and the shallow potential well characteristic of the dielectric screening.

Although we have concentrated on Na-doped $(CH)_x$ to this point, and structural details are undoubtedly different for $(CH)_x$ with other dopants, it is not unreasonable that 4–6 % doping will lead to similar well depths and the insulator-metal transition for other donors. This will be discussed further in Sec. IV. However, very similar behavior has been found for ClO_4^- doping, with an insulator-metal transition at $\sim 6\%$, and $\eta(E_F)=0.08$ states/eV C-atom in the metallic state.[3] We show now that this can be explained in close analogy with our explanation for donor-doped material. For acceptor doping, the solitons are positively charged and the midgap soliton band found when the Coulomb potential is neglected is completely empty, i.e., filled with holes. V_n is positive rather than negative in this case and the potential well is inverted to become a barrier. A plot of the energy levels versus the fraction of V_n in this case would show them tending to rise rather than fall. As the potential energy increases, the lowest-energy states in a band and, in particular, the lowest-energy states in the soliton band, will tend to become concentrated toward the ends of the chain, rather than in the center as for donor doping. When the potential has increased far enough, they will no longer continue to rise in energy with increasing V_n as do the remainder of the states in the band, which will therefore separate from them. In analogy to the n-type case the insulator-metal transition will occur when the valence-band states rise sufficiently to have closed the gap between them and the lowest soliton states. The hole wave functions in the latter states will at this point have again spread over the chain, and hole conduction can take place in the resulting band.

It should be noted that the calculated band structure is not independent of boundary conditions because they affect the well depth. This will not matter much for the insulator side of the transition, because the gap changes are so small anyway for 6.67% doping, but they could be quite significant for the metallic side. The boundary conditions for the case illustrated in Figs. 4 and 5 were, to a great extent, determined by the fact that the outermost ions and the solitons bound to them were opposite sites 8 and 100. Due to the strong screening their potentials were small at the beginning of the chain, as seen in Fig. 4, and thus made full contribution to the depth of the well. The minimum distance of an ion from the end of the chain should be l, or about five sites; a shorter distance would not give rise to a stable soliton-ion configuration. If the outermost ions had been at sites 5 and 103, the well depth would have been smaller by ~ 0.2 eV. As can be deduced from Fig. 5, such a decrease in depth would have had a noticeable effect, increasing the gap and decreasing $\eta(E_F)$ somewhat. Because the gap decreases with increasing chain length, self-consistency and the metallic state could still have been achieved by going to a chain with two more solitons, or 24 more sites.

It would also be possible to have deeper wells for a given chain length than has been considered above. These could be created, for example, by one or more of the ions giving up its electron to an impurity elsewhere, thus decreasing the number of negatively charged solitons on the surrounding chains. This could result in a chain shorter than 108 sites becoming metallic. In practice, one would expect a variety of boundary conditions to occur in any given sample. What our calculation has demonstrated is that the insulator-metal transition occurs for one plausible set of boundary conditions at a reasonable chain length. It appears that this should still be true for a range of boundary conditions. In any case, not all of the sample becomes metallic.

We conclude this section with a brief discussion of some of the approximations and omissions in our model. The use of a single-chain calculation, or basically a one-dimensional model, appears justified by the observation of the soliton IRAV in metallic samples, plus the large anisotropy found in the conductivity of oriented metallic samples.[39] Nevertheless, interchain interactions might smear out the level structure we have calculated, decreasing the gaps. Another possible source of error is the use of fixed soliton spacing, i.e., Eq. (2), rather than allowing

the chains to relax. In calculations for a well with depth increasing to a maximum at the center, when the chains were allowed to relax the solitons were found to be shorter around the center of the well, corresponding to the expected larger electron concentration there. Little error is expected from this source in the present calculation, however, because as seen in Fig. 4 the average V_n in the well is quite flat except for a few sites at the ends. The rapid increase in V_n at the ends might cause a spreading of the end solitons, but this is not likely to have much effect on the energy levels. The neglect of electron-electron interactions on the chain might be serious on the insulator side of the transition. It should not be important on the metal side, where screening along the chain should be quite good. On the insulator side, however, the very approximate treatment of the screening must be a more important source of error than neglect of electron-electron interactions. In any case, all these considerations are unlikely to affect the conclusion that the gap is little changed for 6.67% doping and for 8.33% doping of very short chains.

III. MAGNETIC SUSCEPTIBILITY

To calculate the magnetic susceptibility χ provided by the π electrons in our model, we derive an expression for χ valid for nonuniform level spacing, including spacing large compared to kT. For an assembly of electrons in a magnetic field of induction B, the numbers per unit volume with spin parallel or antiparallel to B are given by N_+ and N_-, respectively, where

$$N_\pm = \tfrac{1}{2}\sum_i{}' f(E_i \mp \mu_B B) \ . \tag{7}$$

Here, f is the Fermi-Dirac distribution, μ_B the Bohr magneton, and the prime indicates that the summation over i is over the states of both spin orientations in a unit volume. Because $kT \gg \mu_B B$ for the usual magnetic fields applied, f is well approximated by

$$f(E_i \mp \mu_B B) \simeq f_i^0[1 \pm (1-f_i^0)\mu_B B/kT] \ , \tag{8}$$

where f_i^0 is the distribution in the absence of a magnetic field. This leads to

$$\chi = \frac{\mu_B(N_+ - N_-)}{B} = 2\frac{\mu_B^2}{kT}\sum_i f_i^0(1-f_i^0) \ , \tag{9}$$

where now the summation over i is over all the energy levels of the distribution in unit volume in the absence of the magnetic field. In this form, Eq. (9) is valid for arbitrary level spacing. In the limit that the density of states at E_F is large, in the present case the long-chain limit, Eq. (9) yields the familiar result for the Pauli susceptibility of a metal, $\chi_P = \mu_B^2 \eta_V(E_F)$, $\eta_V(E_F)$ representing the density of states at the Fermi energy in unit volume for both spins. For the polymers it is usual to express χ in emu/mol. In that case χ may be written

$$\chi(\text{emu/mol}) = (3.24\times 10^{-5})\eta(E_F) \ , \tag{10}$$

where $\eta(E_F)$, the number of states of both spins/eV C-atom, is given, according to Eq. (9), by

$$\eta(E_F) = 2\sum_i f_i^0(1-f_i^0)/NkT \ . \tag{11}$$

Here, kT is in units of eV and the summation i is over the states (either spin) of a chain of N C-H's. The loss of the temperature dependence of $\eta(E_F)$ in a metal is due to $f^0(1-f^0)$ being proportional to kT.

The general behavior of χ predicted by Eqs. (9)–(11) is clear. If the gap 2Ω between the highest occupied and lowest empty level is large compared to kT, only these two levels can contribute to χ. With E_F lying halfway between the two levels in this situation, the equations lead to $\chi \propto [\exp(-\Omega/kT)]$. As seen earlier, 2Ω depends on the length of the doped chain, L_d. For the smallest L_d, corresponding to two solitons, $2\Omega \gg kT$. As shown in the preceding section, for 8.33% doping, 2Ω decreases with increasing L_d, with the result that χ increases, exponentially at first and then less rapidly when, with increasing doping, 2Ω becomes comparable to kT. In the limit of large L_d and sufficient overlap of adjacent solitons, χ should reach a saturation. It will be shown now that these considerations can account for the observed variation of χ_P with y.

The variation of χ_P with y for Na doping is given in Fig. 6 of Ref. 2. For the samples of that study it is clear that up to $\langle y \rangle \sim 5\%$, at least, the part of the sample in the Na-rich phase must have $y = 6.67\%$ or $b = 15$. According to Eq. (9) and the results of our band-structure calculations, for $b = 15$ χ depends exponentially on Ω and $1/T$ for all reasonable chain lengths, remaining well below 10^{-8} emu/mol, the upper limit found experimentally, below $\langle y \rangle \sim 5\%$.[2,4] We identify the doping concentration at which χ_p is observed to begin increasing, $\langle y \rangle = 0.055$ or 0.056,[2] as the concentration where the 8.33% phase is beginning to build up. (We note that part of the sample is generally undoped[33] and it is, in any case, difficult to determine $\langle y \rangle$ accurately.) At $\langle y \rangle = 0.060$, χ_P has increased to between $\frac{1}{3}$ and $\frac{1}{2}$, according to the error bars in Ref. 2, of the maximum measured value. With 0.060 representing an increase in ion concentration over 0.055 of 7% or 8%, close to $\frac{1}{3}$ of the 25% increase required to go from $b = 15$ to $b = 12$, it does not appear difficult to account qualitatively for the increase at $\langle y \rangle = 0.060$. This could not be done quantitatively in any case without knowledge of how L_d builds up with increasing $\langle y \rangle$. One factor that could account for an initial rapid rise with increasing doping is the exponential dependence referred to earlier of χ on Ω, which, in turn, decreases rapidly with increasing L_d. Another possible factor stems from the dielectric-constant dependence on the gap. One may speculate that the tendency of the dielectric constant to increase with decreasing gap, decreasing the constant potential, would retard the decrease of the gap with increasing y until y grows sufficiently large in a local region for metallic behavior to be attained locally.

In a number of experimental studies for dopants other than Na, χ_P was also observed to saturate in the high doping limit at $(2-3)\times 10^{-6}$ emu/mol, corresponding to $\eta(E_F) = 0.08-0.09$ states/eV C-atom, the difference being within the error bars. It is of interest, then, whether the

similar values for different samples indicate that they all have average chain lengths ~ 100 sites, or whether η is independent of chain length in the metallic state. We have carried out our calculations of band structure for longer chains and find that the self-consistent η increases slightly, to ~ 0.084 states/eV C-atom at 156 sites, and then decreases slightly, to 0.082 states/eV C-atom at 252 sites. In view of the accuracy of the susceptibility measurements, these results tell us that χ_P is essentially independent of chain length in the metallic state. Thus, in particular, we can predict that χ_P will be essentially unchanged for the higher-conductivity $(CH)_x$ samples made recently,[40,41] despite the presumably longer chains.

It is a consequence of our model that, particularly for chain lengths of ≤ 100 sites, properties that depend on the level spacing in the neighborhood of E_F, such as χ_P, will be temperature dependent because the level spacing is not small compared with kT. One type of study that reveals temperature dependence of the insulator-metal transition is that of the ESR linewidth.[28] It has been demonstrated by a number of groups that the ESR linewidth at 300 K changes dramatically around $\langle y \rangle \sim 5\%$.[2,3,28] Bernier and co-workers have also shown that in samples with $\langle y \rangle > 5\%$ the nature of the temperature dependence of the linewidth changes at low temperatures. At high temperatures the ESR linewidth for these samples increases with temperature, as is usually observed for metals where the spin-lattice-relaxation rate is controlled by spin-orbit coupling. Below ~ 50 or 100 K, however, the linewidth decreases with increasing temperature, as expected for a semiconductor.[28]

The temperature dependence of χ_P, from which the gap could be deduced, is not easily obtained from magnetic-susceptibility measurements because the measured χ is a sum of the core susceptibility, a Curie contribution χ_C due to localized defects with spin, and χ_P. Although the core susceptibility is readily subtracted out, it is not entirely straightforward to separate in the remaining χ, denoted χ_{spin}, χ_C and χ_P when both are temperature dependent. At low temperatures, for many highly doped samples, χ_{spin} has been found to show the $1/T$ dependence characteristic of Curie spins.[42–44] With increasing temperature, the $1/T$ region goes over into a plateau or T-independent region. The plateau may persist to room temperature or may go into a region of positive slope with increasing T. The latter behavior, found in iodine,[42] ClO_4,[43] and AsF_5-doped[44] samples at y values in the neighborhood of the insulator-metal transition, can only indicate an increase in χ_P with increasing temperature. Such an increase is expected from the foregoing theory for $2\Omega > kT$. Epstein *et al.* find that $\chi_P(T)$ for an iodine-doped sample close to the transition ($\langle y \rangle = 0.444$) can be fitted by an exponential corresponding to a gap $2\Omega = 0.11$ eV.[42] This temperature dependence is quite close to what we obtain from our model for $L_d \simeq 100$. Although our calculations were not done for iodine doping, the observation of such a temperature dependence for χ_P is significant evidence for our theory. As will be discussed further in Sec. IV, however the dopant reorganizes the lattice, the effect of the ion potential must be to modify the density of states more or less as has been found for the Na case.

It should be noted that Ikehata *et al.*, who also measured χ_{spin} versus T for AsF_5 doping, did not find any T dependence for χ_P; this was the result of assuming a T-independent χ_P in deconvoluting their data.[45] Moraes *et al.* also claim that χ_P is T independent for $\langle y \rangle$ above the insulator-metal transition.[2] That claim is, however, not warranted by the data they present. Indeed, they show that the total χ is independent of T down to ~ 45 K for $y = 0.057$, where the sample is barely into the insulator-metal transition. The 300-K χ for this sample is quite small, only about twice the constant background χ_C documented by data points from $y = 0.003$ to $y = 0.045$. In interpreting the total χ for the 0.057 sample as χ_P, Moraes *et al.* have assumed that the background χ_C has completely disappeared at $y = 0.057$, but this is in contradiction to what has been seen by others[42–44] in similarly doped samples. It could easily be true that sufficient χ_C remains to keep the value of χ constant down to 45 K, even though χ_P decreases, as predicted by our theory. The spins that cause the background χ_C might be neutral defects present in regions inaccessible to the dopant ions, because the latter must diffuse accompanied by a soliton or polaron. An example of such a region would be a very short chain terminated by chain breaks or sp^3 defects.

IV. SAMPLE AND DOPANT DEPENDENCE OF THE METAL-INSULATOR TRANSITION

The detailed variation of χ_P with y is quite sample dependent. That makes it difficult to decide whether χ_P is also dopant dependent; that question will be discussed later in this section. Sample dependence is probably largely due to nonuniformity of the doping, i.e., beyond what is the result of a two-phase model. In the case of iodine, for example, it has been found that rapid doping[42] can result in the surface regions of the fibrils being doped into the metallic range before the iodine penetrates into the interior.[46,42] Even a more careful, slow-doping procedure can result in nonuniformity. χ_P for slow-doped samples was found to reach a value of about one-tenth the metallic value for $y < 1\%$,[42] again suggesting surface metallic regions. Still, this increase was followed by a plateau of χ_P versus increasing y that persisted to the beginning of the steep increase to the full metallic value at $\sim 4\%$, consistent with the doped regions that grew up between 1% and 4% being too small to be metallic. Indeed, Pouget found, by x-ray analysis, that for this range of iodine doping "the coherence length ~ 25 Å does not change appreciably with $\langle y \rangle$, which means that doping occurs mainly by multiplication of small aggregates which remain structurally uncorrelated as $\langle y \rangle$ increases."[9] These observations suggest that the variation of χ_P with $\langle y \rangle$ can be used to obtain information on the growth of the dopant-rich phase.

In contrast to the iodine case, for the Na-doped samples that we have been discussing the variation of χ_P with y indicates that the 6.67% phase was established

throughout (except for $\sim 10\%$ presumably undopable portions of the sample) before the buildup of the 8.33% phase began. It should be pointed out that achieving such uniformity of doping requires special samples—with small-thickness and small-diameter fibrils (100 Å for these samples)—as well as attention to the doping procedure.[2-4] More recently, results for ClO_4 doping similar to those for Na doping have been obtained.[3] In the new data the sharp increase in χ_P occurs at ~ 6–7%, rather than at $\sim 4\%$ as found earlier.[44]

Uniformity of doping is also affected by the concentration of conjugation-interrupting defects such as sp^3 inclusions. Such defects can stop the motion of polarons or solitons accompanying the diffusing ions and thus cause a break in the doping. We conclude from this discussion that, because of nonuniformity of doping and defects, including amorphous regions, the $\langle y \rangle$ value at which χ_P begins an abrupt rise may be considerably diminished from the value in homogeneous material.

Although, in principle, the evolution of the band structure with $\langle y \rangle$ might be quite different for different dopants, there is some evidence that the differences are small in practice. One piece of evidence is the insensitivity of the shape and position of the midgap optical absorption to dopant type.[1] Optical absorption in the metallic phase is also quite similar for different dopants, notably Na (Ref. 2) and ClO_4,[3,7] which lead to quite different geometric structures. Another piece of evidence for similar band structure in the metallic state despite different geometric structure is the fact, noted earlier, that the saturation value of χ_P is about the same, leading to $\eta(E_F)$ of 0.08 or 0.09 states/eV *C*-atom, for the common dopants. Interestingly, there is some evidence that the metallic phase corresponds to $y \sim 8\%$, or an average of 12 sites between donated electrons or holes, for a number of dopants, notably I_3, ClO_4^-, $FeCl_4^-$, and several other tetrahedral acceptors, just as it does for Na. This is a correlation to be expected, perhaps, because a determinant of metallic behavior should be the overlap of electron or hole soliton wave functions. The structure of the metallic phase for the common acceptors appears to be determined by their size being comparable to one of the spacings between $(CH)_x$ chains. A common feature of acceptor doping revealed by x rays is a long interplanar spacing corresponding to the sum of the diameter of a $(CH)_x$ chain and the size of the acceptor molecule.[9,47] This feature is consistent with a structure in which dopant-rich planes alternate with $(CH)_x$ planes.[9] 8% doping would correspond to the dopant-rich planes consisting of half $(CH)_x$ columns and half dopant columns.[9] Alternation of $(CH)_x$ and dopant columns would be expected because it reduces the Coulomb repulsion between the ion columns. More direct evidence for such a structure of the metallic phase in the case of $FeCl_4^-$ doping is the fact that the doping is found to be fully homogeneous, i.e., the material is single phase, at $\sim 8\%$ doping.[48] In the case of I_3^- doping the concentration in the metallic phase has been deduced from a comparison of the intensity of the diffraction lines from a sample of pure *trans*-$(CH)_x$ and a slowly doped sample from the same initial film with 12.5% I.[49] The ratio of the intensities showed that about 50% of the doped sample was actually not doped. This implies that the concentration of I in the doped phase is 25%, or $\sim 8\%$ I_3^-.

V. OPTICAL ABSORPTION

In undoped polyacetylene optical absorption is very small below ~ 1.4 eV, and then rises rapidly with increasing photon energy, peaking at 1.9 or 2.0 eV.[1] It is now realized that the gap is ~ 1.8 or 1.9 eV, the strong absorption below that energy being due to the creation of soliton-antisoliton pairs[50-52] or breather modes.[53] Thus the peak at ~ 2 eV corresponds to valence-band edge to conduction-band edge transitions. With small doping, $\sim 0.4\%$, a broad flat absorption arises within the gap, extending to 1.4 eV with a very gentle maximum at ~ 0.7 eV.[1,2] This absorption grows in magnitude, maintaining its shape, as the doping increases, while the 2-eV peak decreases in magnitude and flattens.[1,2,7] Finally, for y in the neighborhood of the metal-insulator transition and beyond it, the 2-eV peak is gone and the absorption decreases monotonically with photon energy from 0.7 to 2.5 eV, the highest energy for which data are generally given.[1,2,7]

It is readily seen that the band structures calculated in Sec. II can account qualitatively for the changes in optical absorption with doping. For Na doping, as discussed earlier, for $0.4 \leq \langle y \rangle \lesssim 5\%$ the doped regions have $y = 6.67\%$. At this concentration the band structure was found to be not much affected by the Coulomb potential. The band structure is then reasonably described as having a number of localized soliton levels equal to the number of ions, distributed symmetrically around midgap according to the SSH Hamiltonian. An example of this structure for eight solitons is shown on the left-hand side of Fig. 5, i.e., for zero Coulomb potential. This type of band structure would give quite a wide absorption in the gap, starting at a few tenths of an eV, with some structure visible. The continuous appearance of the optical absorption, without structure, is due to the superposition of the absorption spectra of chains with differing energy levels as a result of different numbers of solitons, different lengths, and probably different boundary conditions. The latter effect would probably also extend the range of absorption. We suggest that the gentle maximum independent of doping arises from a greater concentration of levels around midgap due to short chains and chains with few solitons. Actually, of course, the peak is at 0.7 eV rather than midgap. That is presumably due to Coulomb effects, specifically electron-electron interactions, which have not been included in our Hamiltonian. The flattening and decrease in the peak absorption at 2 eV with increasing doping arises because the soliton levels are created at the expense of the large densities of states at the valence- and conduction-band edges.

For $\langle y \rangle \geq 6\%$, or past the metal-insulator transition, in Na-doped $(CH)_x$ the 8.33% phase is expected to be predominant. We note that, although there are no longer localized levels (except at the very bottom and top of the

π band), the selection rule for **k** will not restrict transitions because the potential is not periodic. In addition to the IRAV, there will now be low-energy transitions from the highest occupied levels to what was the conduction band, and continuous absorption beyond that (see Fig. 5). As in the 6.67%-doping region, any possible structure in the absorption would be smeared out because of different numbers of solitons on a chain, different chain lengths, and different boundary conditions for different chains. For Na-doped[2] and ClO_4-doped[7] material close to the transition, there is still a peak at ~ 0.7 eV, but the peak in I_3^--doped material for $\langle y \rangle$ above, but close to, the transition, is at ~ 0.3 eV.[54] It may be that in this range of doping the detailed variation of the absorption with photon energy depends on the details of growth of the doped chain length as $\langle y \rangle$ increases.

VI. CONCLUSIONS

From our calculations we conclude that the conditions required for doped $(CH)_x$ to show metallic susceptibility are (1) donated electrons (holes) in soliton states; (2) sufficient chain length so that the average spacing between levels is $\lesssim kT$; (3) small enough ion spacing so that the wave function of electrons (holes) on adjacent solitons overlap; and (4) high enough donor (acceptor) doping so that there is a deep potential well (barrier). Using the SSH Hamiltonian plus the Coulomb potential of the ions and charged solitons, with screening treated carefully, we have shown that these conditions are met for Na-doped $(CH)_x$ with ion spacing $4a$, corresponding to 12 sites between solitons (8.33% local doping) and a chain length of $\gtrsim 100$ sites. There are indications that metallic behavior corresponds to $\sim 8\%$ local doping for a variety of other dopants as well. It has been shown that our model is consistent with the observed saturation Pauli susceptibility, the variation of χ_P with doping, and the optical absorption of doped $(CH)_x$. Detailed calculations of χ_P variation for very short chains with 8.33% doping have not been done, because they would require a more careful treatment of screening for the semiconducting case, including the contribution of solitons and perhaps free electrons in the conduction band, and a self-consistent one.

It is clear from the preceding discussion that the insulator-metal transition in polyacetylene is best described as a Mott transition. The features that give the transition the appearance of being first order arise from the characteristics of the ion distribution. The sharp increase in χ_P for Na-doped $(CH)_x$ at $\langle y \rangle \sim 6\%$ is due to the ion concentration, having achieved 6.67% (spacing $5a$) throughout the dopable regions of the sample, suddenly starting to increase locally from 6.67% to 8.33% (spacing $4a$). The other characteristic cited as indicative of a first-order transition is the hysteresis observed for χ_P.[2] This also is clearly attributable to the ions, specifically to the hysteresis of ion insertion and withdrawal due to kinetic limitations. This hysteresis has been well documented in studies of K and Na doping,[55,33] which show, for example, that the stable phases observed are different for ion insertion and ion withdrawal.

A significant consequence of our model is that the metal-insulator transition is temperature dependent as well as dopant-concentration dependent. The degree of temperature dependence depends on the doped chain length and perhaps on the degree of doping. For samples with $\langle y \rangle$ not far above the transition, where L_d would be close to the minimum value compatible with metallic behavior at 300 K, we have quoted experimental results for χ_P that show a semiconducting gap of ~ 0.1 eV below 300 K.[42] In samples with larger $\langle y \rangle$, L_d could be larger, resulting in smaller spacing between levels and therefore a smaller gap. It is also possible that for larger $\langle y \rangle$ a new phase with smaller ion spacing, and therefore larger wave-function overlap, could arise, which would also have a smaller gap. It is in any case true that χ_P was found to be less temperature dependent for samples with sufficient iodine doping to be well past the transition.[41] In principle, for long enough chains, doped $(CH)_x$ could be metallic down to extremely low temperatures.

[1] See, for example, A. Feldblum, J. H. Kaufman, S. Etemad, A. J. Heeger, T. -C. Chung, and A. G. MacDiarmid, Phys. Rev. B **26**, 815 (1982).

[2] F. Moraes, J. Chen, T. -C. Chung, and A. J. Heeger, Synth. Met. **11**, 271 (1985).

[3] J. Chen and A. J. Heeger, Synth. Met. **24**, 311 (1988).

[4] J. Chen, T. -C. Chung, F. Moraes, and A. J. Heeger, Solid State Commun. **53**, 757 (1985); T. -C. Chung, F. Moraes, J. D. Flood, and A. J. Heeger, Phys. Rev. B **29**, 2341 (1984).

[5] E. J. Mele and M. J. Rice, Phys. Rev. B **23**, 5397 (1981).

[6] W. P. Su, Solid State Commun. **42**, 497 (1983).

[7] X. Q. Yang, D. B. Tanner, M. J. Rice, H. W. Gibson, A. Feldblum, and A. J. Epstein, Solid State Commun. **61**, 335 (1987).

[8] R. H. Baughman, N. S. Murthy, G. G. Miller, L. W. Shacklette, and R. M. Metzger, J. Phys. (Paris) Colloq. **44**, C3-53 (1983); R. H. Baughman, L. W. Schacklette, N. S. Murthy, G. G. Miller, and R. L. Elsenbaumer, Mol. Cryst. Liq. Cryst. **118**, 253 (1985).

[9] J. P. Pouget, in *Electronic Properties of Polymers and Related Compounds*, edited by H. Kuzmány, M. Mehring, and S. Roth (Springer-Verlag, New York, 1985) p. 26.

[10] S. Kivelson and A. J. Heeger, Phys. Rev. Lett. **55**, 308 (1985).

[11] S. Etemad, A. Pron, A. J. Heeger, A. J. MacDiarmid, E. J. Mele, and M. J. Rice, Phys. Rev. B **23**, 5137 (1981).

[12] E. J. Mele and M. J. Rice, Phys. Rev. Lett. **45**, 926 (1980).

[13] D. Tanner, G. Doll, K. Rao, M. H. Yang, C. Eklund, G. Arbuckle, and A. G. MacDiarmid, Bull. Am. Phys. Soc. **32**, 422 (1987).

[14] H. -Y. Choi and E. J. Mele, Phys. Rev. B **34**, 8750 (1986).

[15] J. C. Hicks, J. T. Gammel, H. -Y. Choi, and E. J. Mele, Synth. Met. **17**, 57 (1987).

[16] J. Fink, N. Nucker, B. Scheerer, A. vomFelde, and G. Leising, in *Electronic Properties of Conjugated Polymers*, edited by H. Kuzmány, M. Mehring, and S. Roth (Springer-Verlag, New York, 1987), p. 94.

[17] B. Horovitz, Phys. Rev. Lett. **46**, 742 (1981).

[18]M. Grabowski, K. R. Subbaswamy, and B. Horovitz, Solid State Commun. **34**, 911 (1980).

[19]Soliton or polaron spacing decreasing continuously with increasing y has also been assumed in the valence effective Hamiltonian (VEH) band-structure calculations of S. Stafström and J. L. Brédas, Phys. Rev. **38**, 4180 (1988).

[20]G. W. Bryant and A. J. Glick, Phys. Rev. B **26**, 5855 (1982).

[21]See also J. P. Albert and C. Jouanin, J. Phys. (Paris) Colloq. **44**, C3-387 (1983).

[22]J. L. Brédas, B. Théman, J. G. Fripiat, J. M. André, and R. R. Chance [Phys. Rev. B **29**, 6761 (1984)] did explicitly include the donor ions (Li^+ or Na^+) in their calculations of the band structure of doped polyparaphenylene. They found that even at 100% doping a gap of 1 eV remained between conduction and valence bands. This result is in contradiction to electron-energy-loss and other experiments on Li-doped polyparaphenylene, which showed the gap to have disappeared at 50% doping [J. Fink, B. Scheerer, M. Stamm, B. Tieke, B. Kannellakopulos, and E. Dornberger, Phys. Rev. B **30**, 4867 (1984)]. We suggest that the incorrect result is due to calculating for an infinite chain, in essence, thus neglecting the existence of a potential well.

[23]B. R. Bulka, Synth. Met. **24**, 41 (1988), and references therein.

[24]E. Conwell and S. Jeyadev, Phys. Rev. Lett. **61**, 361 (1988).

[25]C. -S. Neumann and R. von Baltz, Phys. Rev. B **35**, 9708 (1987).

[26]W. Ottinger, G. Leising, and H. Kahlert, in *Electronic Properties of Polymers and Related Compounds,* edited by H. Kuzmány, M. Mehring, and S. Roth (Springer-Verlag, New York, 1985), p. 63.

[27]See, for example, J. M. Ziman, *Principles of the Theory of Solids,* 2nd ed. (Cambridge University Press, Cambridge, 1972), pp. 161–163.

[28]P. Bernier, A. El-Khodary, F. Rachdi, and C. Fite, Synth. Met. **17**, 413 (1987).

[29]W. P. Su, J. R. Schrieffer, and A. J. Heeger, Phys. Rev. B **22**, 2099 (1980); **28**, 1138(E) (1983).

[30]M. Winokur, Y. B. Moon, A. J. Heeger, J. Barker, D. C. Bott, and H. Shirakawa, Phys. Rev. Lett. **58**, 2329 (1987).

[31]N. S. Murthy, L. W. Shacklette, and R. H. Baughman, Bull. Am. Phys. Soc. **31**, 232 (1986).

[32]A. Metrot, D. Guerard, D. Billaud, and A. Herold, Synth. Met. **1**, 363 (1980).

[33]L. W. Shacklette and J. E. Toth, Phys. Rev. B **32**, 5892 (1985).

[34]A. Takahashi and H. Fukutome, Solid State Commun. **62**, 279 (1987).

[35]H. Takayama, Y. R. Lin-Liu, and K. Maki, Phys. Rev. B **21**, 2388 (1980).

[36]R. Resta, Phys. Rev. B **16**, 2717 (1977).

[37]C. G. Kuper, Phys. Rev. **150**, 189 (1966).

[38]D. Davis, Phys. Rev. B **7**, 129 (1973).

[39]See, for example, Y. W. Park, C. Park, Y. S. Lee, and C. O. Yoon, Solid State Commun. **65**, 147 (1988).

[40]N. Basescu, Z.-X. Liu, D. Moses, A. J. Heeger, H. Naarmann, and N. Theophilou, Nature (London) **327**, 403 (1987).

[41]N. Theophilou, D. B. Swanson, A. G. MacDiarmid, A. Chakraborty, H. H. S. Javadi, R. P. McCall, S. P. Treat, F. Zuo, and A. J. Epstein, Synth. Met. **28**, D35 (1989).

[42]A. J. Epstein, H. Rommelmann, M. A. Druy, A. J. Heeger, and A. G. MacDiarmid, Solid State Commun. **38**, 683 (1981).

[43]A. J. Epstein, R. W. Bigelow, H. Rommelmann, H. W. Gibson, R. J. Weagley, A. Feldblum, D. B. Tanner, J. P. Pouget, J. C. Pouxviel, R. Comès, R. Robin, and S. Kivelson, Mol. Cryst. Liq. Cryst. **117**, 147 (1985).

[44]Y. Tomkiewicz, T. D. Schultz, H. D. Brown, T. C. Clarke, and G. B. Street, Phys. Rev. Lett. **43**, 1532 (1979).

[45]S. Ikehata, J. Kaufer, T. Woerner, A. Pron, M. A. Druy, A. Sivak, A. J. Heeger, and A. G. MacDiarmid, Phys. Rev. Lett. **45**, 1123 (1980).

[46]A. Janossy, L. Pogany, S. Pekker, and R. Swietlik, Mol. Cryst. Liq. Cryst. **77**, 185 (1981).

[47]Such a feature is also reported for AsF_5 doping by C. Riekel, H. W. Hässlin, K. Menke, and S. Roth, J. Chem. Phys. **77**, 4254 (1982).

[48]J. P. Pouget, A. Pron, A. Murasik, D. Billaud, J. C. Pouxviel, P. Robin, I. Kulszewicz, D. Begin, J. J. Demai, and S. Lefrant, Solid State Commun. **57**, 297 (1986).

[49]P. Robin, J. P. Pouget, R. Comès, H. W. Gibson, and A. J. Epstein, J. Phys. (Paris) Colloq. **44**, C3-87 (1983); Polymer **24**, 1558 (1983).

[50]J. P. Sethna and S. Kivelson, Phys. Rev. B **26**, 3513 (1982).

[51]A. Auerbach and S. Kivelson, Phys. Rev. B **33**, 8171 (1986).

[52]J. Yu, H. Matsuoka, and W. P. Su, Phys. Rev. B **37**, 367 (1988).

[53]B. Horovitz, A. R. Bishop, and S. R. Phillpot, Phys. Rev. Lett. **60**, 2210 (1988).

[54]A. J. Epstein, R. W. Bigelow, A. Feldblum, H. W. Gibson, D. M. Hoffman, and D. B. Tanner, Synth. Met. **9**, 155 (1984).

[55]L. W. Shacklette, N. S. Murthy, and R. H. Baughman, Mol. Cryst. Liq. Cryst. **121**, 201 (1985).